

Mapping the distribution of sea urchin (Echinoidea) and benthic habitat using drone in the waters of Lancang Island

Muhammad Sony Sastraantara^{1*}, Syamsul Bahri Agus², and Setyo Budi Susilo²

¹Graduate School of Marine Technology, Faculty of Fisheries and Marine Science, IPB University, Jalan Agatis, Kampus IPB Dramaga, Bogor, 16680, West Java, Indonesia

²Department of Marine Science and Technology, Faculty of Fisheries and Marine Science, IPB University, Jalan Agatis, Kampus IPB Dramaga, Bogor, 16680, West Java, Indonesia

Abstract. Sea urchins are valuable marine creatures that live in the waters of Indonesia, and typically found in seagrass and coral reefs. This study aimed to determine the distribution of sea urchins and the benthic characteristics that serve as their habitat using high resolution drone images. Object-based image analysis (OBIA) with a support vector machine algorithm is used to identify benthic habitats, while the distribution of sea urchins is determined by thresholding pixel values. A total of 812 aerial photos with a spatial resolution of 3.98 cm/px were obtained and mapped into five classes of benthic habitat (sand, rubble, seagrass, living coral, and dead coral algae). The dominant habitat class obtained was dead coral algae, with an area of 234,035 m² (29.63%), whereas seagrass was the smallest, with an area of 74,149 m² (9.39%). The overall accuracy of the benthic classes was 65.44%, with kappa coefficient value of 0.57. The study found that the total number of sea urchins on Lancang Island was 61,551. The dominant distribution of sea urchins was found in the living coral class with 18,094 individuals, but the highest density was in the rubble class with 1358 individuals/ha.

1 Introduction

Sea urchins are invertebrate animals with a body shape resembling a ball with a hard and spiky shell. In some species, they are black in color. Sea urchins are commonly found in seagrass beds and coral reefs in clear and calm waters [1]. Sea urchins are organisms that driven shallow-water community system because of their specific relationship with various benthic habitats [2]. The sea urchins move using tube feet. Based on several studies, the movement of sea urchins is limited (sedentary). The *Paracentrotus lividus* sea urchin moved 379 cm with a starting point of 150 cm over a study period of 3 months. Meanwhile, the movement of *Diadema antillarum* sea urchins was only 0-5 meters in 4 h, with a pattern of circular movement returning to the starting point [3]. In animals with limited movement, the distribution of sea urchins in the water body can be detected using remote sensing technology.

* Corresponding author: sonysony@apps.ipb.ac

Remote sensing technology has been widely used to map benthic habitats [4]. The benthic habitat is composed of seagrass, live coral, dead coral, and algae, with substrate types such as sand, rubble, and mud [5], where it serves as the living environment for sea urchins. Remote sensing is an effective method for gathering information on benthic habitats in vast areas [6]. Drones are among the technologies used in remote sensing. Drones have become an alternative to fulfill the needs of mapping and detecting objects with high spatial resolution and less cloud cover [7]. Drone technology offers the advantages of high-resolution camera sensors, flexibility, and efficiency in image acquisition at low cost [8]. Therefore, drones are effective tools for detecting marine fauna [9]. The size of a sea urchin reaching only 70 mm [10] makes it detectable only with high spatial resolution, as spatial resolution affects the detection accuracy [11]. Images captured by drones can be classified by object detection using Object-Based Image Analysis (OBIA) [12]. This classification technique is based on the color (tone) and texture of objects in a segmented image [13]. Another method for detecting objects in an image is image thresholding [14]. Image thresholding involves analyzing the object's ratio to separate the digital values of the object from its surrounding environment [15]. In cases where the color differentiation between the object and its surrounding environment is not sufficiently distinct, image processing is employed to enhance the contrast of the object [16]. Several studies have been conducted to compare benthic habitat mapping using drones and satellite imagery, and the results showed that drone accuracy is higher than satellite imagery [17]. Several studies have shown that the properties of light that penetrate water, such as water depth and sunlight reflection (sunlight), influence the detection of marine fauna. Therefore, research can only be conducted in shallow waters by adjusting the camera angle such that it is not affected by sunlight [18]. The purpose of this study was to map the distribution of sea urchins on Lancang Island based on the benthic habitats in which they live.

2 Material and methods

2.1 Study area

The research was conducted in the waters of Lancang Island, Seribu Islands, and DKI Jakarta. This involved the utilization of 30 virtual transects based on field observations targeting the presence of sea urchins. The virtual transect area is 10 square meters. Additionally, the study encompassed a comprehensive survey of the entire Lancang Island area to acquire information on benthic habitats. The data collection phase took place from February to 13-18, 2023, with 197 classification points and 209 benthic habitat accuracy points. The study area is illustrated in **Fig. 1**.

2.2 Tools and data

The data used are the result of field data collection, such as aerial photos and tagging data (sea urchin and benthic habitat). Aerial photo data were captured using a DJI Mavic Pro drone with the DroneDeploy application. Tagging data were collected using Garmin 66s handheld GPS. Aerial data processing was performed using the Agisoft software, followed by image processing using ArcGIS, ENVI, and eCognition.



Fig. 1. Study location, the Lancang Islands, divided into 3 classes (land, shallow water, and deep water) with 30 sea urchin stations.

2.3 Method

The steps involved in this study are illustrated in **Fig. 2**. The in-situ data collection encompassed aerial photographs, benthic tagging, and sea urchin tagging. Subsequently, the aerial photographs were subjected to photogrammetric processing to generate geometrically corrected images. Following this, an image processing technique involving thresholding of the sea urchins' digital values and classification of benthic habitats using Object-Based Image Analysis (OBIA) based on the tagging results was employed. The outcomes of sea urchin thresholding and benthic habitat classification were overlaid to ascertain the spatial distribution of sea urchins within benthic habitats.

2.4 Field observation

Field observations included capturing aerial photos from a flight path plan. The flight path planning process is performed using DroneDeploy software, which can set the drone flight parameters. Aerial photo data collection in the waters of Lancang Island was conducted from 3:00 PM to 5:00 PM local time (WIB). Sampling data for sea urchins were obtained using random sampling techniques, which involve observing the sea urchin's condition at randomly designated points.

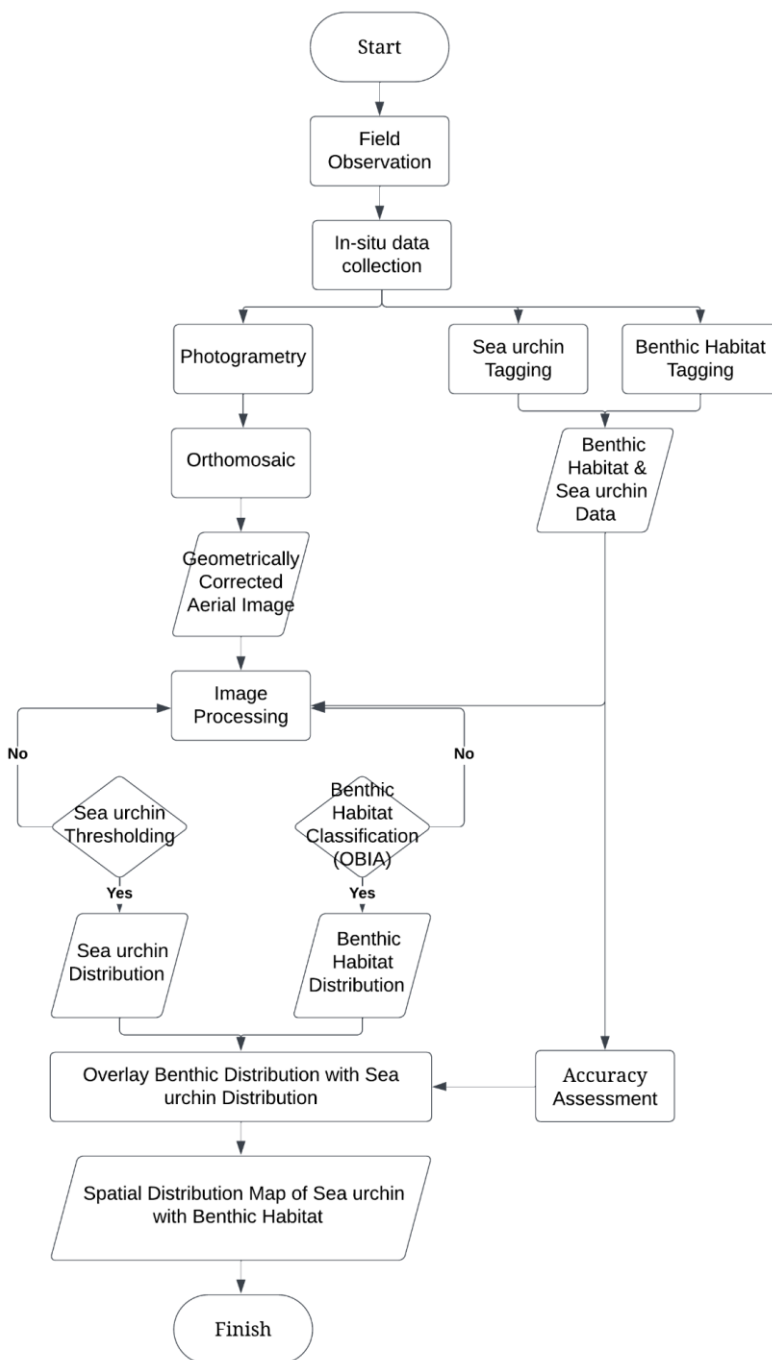


Fig. 2. Research workflow diagram of mapping sea urchin and benthic habitat.

2.5 Flight plan

The flight plan captures aerial photos of the autopilot using the DroneDeploy application. Several parameters were set according to user preferences to produce the desired images. In this study, the parameters were set to a height of 120 m, 70% overlap, flight direction of -39° , flight speed of 13 m/s, and gimbal angle of -90° . The basic flight plan (**Fig. 3**) sets some fundamental parameters, such as altitude and 3D settings, while the advanced flight plan (**Fig. 4**) adjusts more parameters, such as overlap, flight direction, and flight speed.

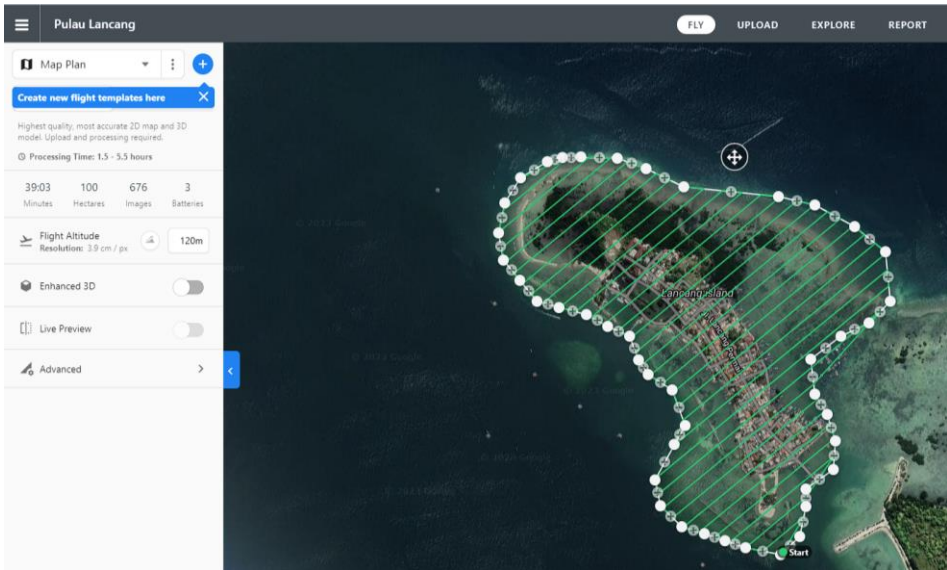


Fig. 3. Basic flight plan with flight altitude set at 120 meters.

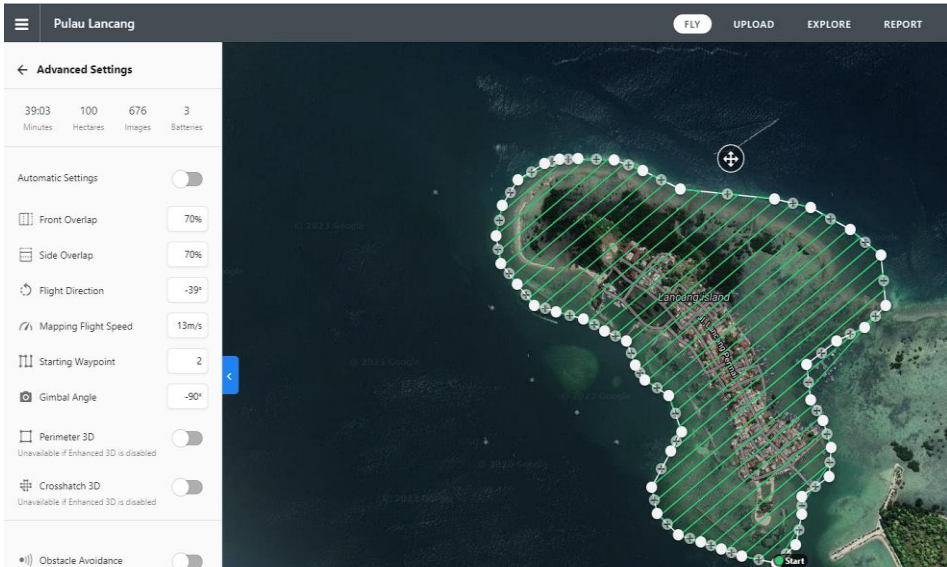


Fig. 4. Advanced flight plan with 70% overlap and -90° gimbal angle.

2.6 Photogrammetry

Photogrammetry combines multiple aerial photos to create an image. The first step is aligning photos, which combines aerial photos by identifying tie points with similar pixel values in each photo. The result of aligning photos is a collection of tied points with x-, y-, and z-values (longitude, latitude, and altitude). The next step is to build a dense cloud to find pixel similarities based on the points in the cloud, resulting in a digital surface model. Subsequently, a mesh was built to construct a surface model based on the dense cloud results, generating a 3D model at the x-, y-, and z-points. The next step is to build a texture and map it by combining photos with the mesh surface. This is performed using the adaptive orthophoto mode, which divides the surface into flat and vertical parts. Subsequently, an orthophoto was created to produce an image based on the photo source and model reconstruction. Once the images were formed, aerial photographs of the waters around Lancang Island were exported. tiff format.

2.7 Image processing

This process is a step to enhance image quality, making it easier to classify benthic habitats and segment sea urchins. Image processing is performed to facilitate segmentation, and contrast stretching is one of the techniques used. Contrast stretching is performed to obtain an image with improved contrast compared with its original form [19]. The primary function of contrast stretching is to enhance the dynamic range of gray levels in an image. An example of the contrast-stretching process is shown in Fig. 5.

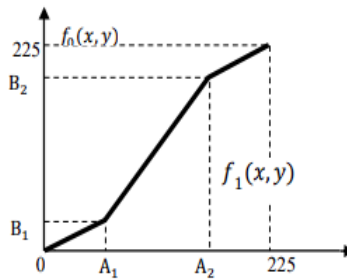


Fig. 5. Contrast stretching transformation illustration.

Description:

- A : Input intensity level;
- B : Output intensity level;
- 255 : Maximum input output intensity level.

If A_1 is equal to A_2 and B_1 is equal to B_2 , then the transformation is in the form of a straight line. This means that there will be no change in the grayscale levels of the resulting image. In general, it is assumed that A_1 is less than or equal to A_2 , and B_1 is less than or equal to B_2 ; therefore, the function will produce a single value, and that value will always increase. The following three functions can be used to calculate the value of the transformation result:

$$\text{For } 0 \leq f_i(x,y) < A_1, f_o(x,y) = f_i(x,y) \frac{B_1}{B_2} \quad (1)$$

$$\text{For } A_1 \leq f_i(x,y) < A_2, f_o(x,y) = B_1 + (f_i(x,y) - A_1) \frac{B_2 - B_1}{A_2 - A_1} \quad (2)$$

$$\text{For } A_2 \leq f_i(x,y) < 255, \text{ then } f_o(x,y) = B_1 + (f_i(x,y) - A_2) \frac{255 - B_2}{255 - A_2} \quad (3)$$

2.8 Image analysis

Image analysis for benthic habitat is performed using the Object-Based Image Analysis (OBIA) method using eCognition Developer. This method is divided into two stages: segmentation and classification. The segmentation process evaluates a set of connected pixels and forms characteristics such as scale, shape, and compactness, referred to as segments. Subsequently, the classification process is carried out to group segments into specific categories based on texture, shape, and pixel values, allowing them to be interpreted as specific properties. Image segmentation employs an algorithm called multiresolution segmentation, which functions by merging single pixel values with neighboring segments [20], creating a heterogeneous threshold value [21].

The multiresolution segmentation algorithm is influenced by the scale, shape, and compactness. The shape of an object influences its spectral similarity and is related to digital values and color. Compactness balances the smoothness of an object when determining its boundaries. Scale affects the level of detail of a segment; the smaller the scale, the more segments are produced with a longer duration. There are no specific rules for adjusting scale, shape, and compactness [22].

The segmentation process is tailored to the object to avoid over- and under-segmentation. Oversegmentation divides an object into more than one segment, whereas undersegmentation results in a segment containing more than one object [23]. The multiresolution segmentation algorithm was applied at two levels at different scales. Level 1 segmentation was performed to determine land, mangrove, shallow sea, and deep-sea areas, whereas level 2 segmentation was conducted to identify benthic habitats. The parameters for Multiresolution Segmentation are listed in **Table 1**.

Table 1. Multiresolution segmentation parameters in eCognition developer.

Level	Class	Parameter
1	Land, Mangrove, Deep Water, Shallow Water	<i>Scale parameter</i> = 1000 <i>Shape</i> = 0.1 <i>Compactness</i> = 0.5
2	Sand, Seagrass, Rubble, Living Coral, Dead Coral Algae	<i>Scale parameter</i> = 200 <i>Shape</i> = 0.1 <i>Compactness</i> = 0.5

In the initial stage, the level 1 image was segmented into various parts, with each part representing specific objects or areas within the image. Subsequently, classification was performed on each of these parts by applying a specific threshold value. The optimal threshold value was obtained by trial and error. For Level 2 classification, the support vector machine (SVM) algorithm was employed as the classifier. The SVM algorithm is a supervised classification method aimed at finding a separating vector between the existing classes by maximizing the margin between these classes. Simply put, the concept of SVM can be explained as an effort to find the best separation line between two classes in the input space [24].

The SVM algorithm is the most effective for classifying benthic habitats compared to other algorithms, such as Bayes, KNN, and DT. The sea urchin images were analyzed using the image threshold value obtained from image processing using Contrast Stretching via ENVI software. This threshold value was then applied to the image to obtain pixels with the specified values. These pixels were then transformed into points to calculate their quantity, which was subsequently overlaid on the benthic habitat image to determine the distribution of sea urchins in relation to the benthic habitat.

2.9 Accuracy assessment

An accuracy assessment was performed by comparing the segmented image with the reference image (ground truth). This accuracy test is known as a confusion matrix. The calculation is provided in [25]. Values for overall accuracy (OA), producer accuracy (PA), and user accuracy (UA). The results of the confusion matrix were then analyzed using the kappa approach to assess the validity and reliability of the research results [26].

3 Results and discussion

3.1 Orthophoto and segmentation

Drone flights were conducted four times to capture aerial photos, resulting in a total of 812 aerial photos. These aerial photos were then processed using orthophoto techniques to generate images of the Lancang Island. An aerial photograph map is shown in **Fig. 6**.



Fig. 6. The aerial image result of merging 812 aerial photos.

The aerial photo acquisition process covers an area of 100 ha, with a flight time of 40 min and a spatial resolution of 3.98 cm/px. In the aerial image of Lancang Island, variations in brightness were observed because of the sun's angle and the camera sensor's ability to focus on an object. Additionally, other weather conditions, such as clouds and wind, also affect aerial photo results and the duration of aerial photo acquisition. The orthophoto results were used for habitat segmentation.

In level 1 segmentation, the multiresolution segmentation algorithm is utilized with a scale value of 1000, shape value of 0.1, and compactness value of 0.5. Level 1 segmentation yields land, mangrove, shallow water, and deep-water classes. In level 2 segmentation, the multiresolution segmentation algorithm was applied with a scale value of 200, shape value of 0.1, and compactness value of 0.5. Level 2 segmentation resulted in classes such as sand, seagrass, rubble, living coral, and dead coral algae. The results of the level 1 and level 2 segmentation are shown in **Fig 7** and **8**, respectively.

The results of the level 1 segmentation were then classified into four classes: land, mangrove, shallow sea, and deep sea, with a land and mangrove area of 33.736 ha (337,360 m²) and a shallow sea area of 78.184 hectares (781,840 m²). A shallow sea area was used for the level 2 segmentation. The level 1 map is shown in **Fig. 7**, while the result of the level 2 segmentation is shown in **Table 2**.



Fig 7. Level 1 segmentation consists of 4 classes (deep water, shallow water, land, and mangrove).

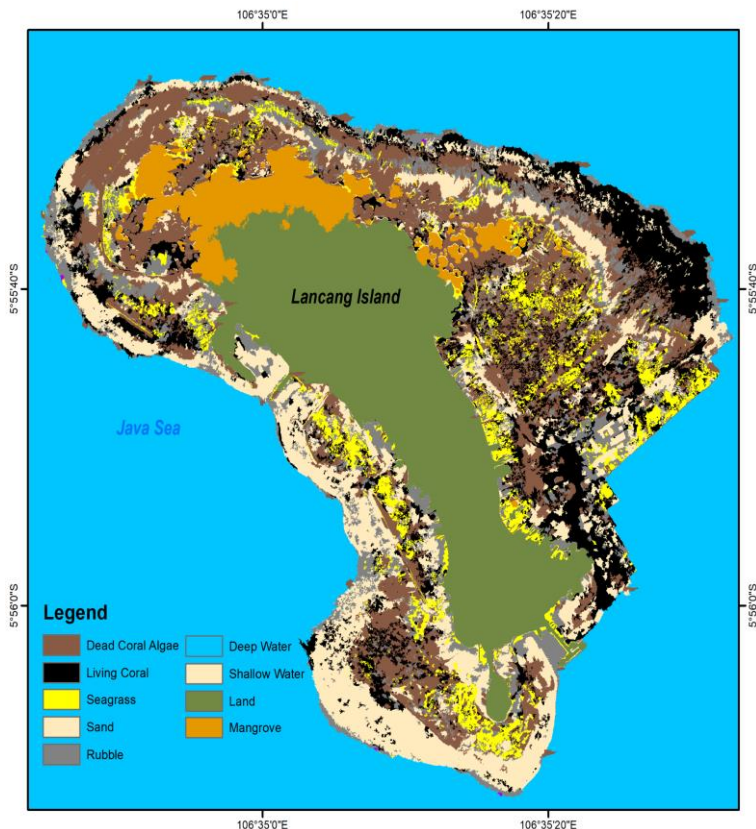


Fig 8. Level 2 segmentation consists of 9 classes (dead coral algae, living coral, dead coral, seagrass, sand, rubble, deep water, shallow water, land, mangrove).

Table 2. Benthic habitat area coverage in Lancang Islands.

Class	Area (ha)	Area (m ²)	Percentage (%)
Sand	18.555	185550	23.49
Seagrass	7.414	74140	9.39
Rubble	13.158	131580	16.66
Living coral	16.457	164570	20.83
Dead coral algae	23.398	233980	29.63
Benthic area	78.982	789900	100

3.2. Benthic habitat accuracy assessment

An accuracy test was conducted using the confusion matrix to obtain values for overall accuracy (OA), producer accuracy (PA), user accuracy (UA), and kappa coefficient. The

overall accuracy is the number of pixels correctly classified for each class compared to the accuracy test samples. The producer accuracy is the average probability of a pixel that has been classified in the field. User accuracy is the pixel that accurately represents a class [27]. The kappa coefficient represents the validity and reliability of the results. The accuracy test results are presented in **Table 3**.

Table 3. Confusion matrix accuracy assessment result for the benthic habitat containing 5 classes.

		Predicted						Total	Ua
		Sand	Rubble	Seagrass	Living coral	Dead coral algae			
Actual	Sand	25	4	5	1	0	35	71.43%	
	Rubble	2	39	3	1	4	49	79.59%	
	Seagrass	3	1	26	0	0	30	86.67%	
	Living coral	0	2	4	21	2	29	72.41%	
	Dead coral algae	13	11	7	12	31	74	41.89%	
	Total	43	57	45	35	37	217		
	Pa	58.14%	68.42%	57.78%	60%	83.78%			
	Oa	65.44%							
Kappa		0.57							

OA = Overall Accuracy, PA = Producer Accuracy, UA = User Accuracy.

Based on **Table 3**, it can be observed that the OA value is 65.44%. The lowest PA value was in the seagrass class at 57.78% and the highest was in the dead algae coral class at 83.78%. The lowest UA value was in the dead algae coral class at 41.89%), and the highest was in the seagrass class at 86.67%). The kappa coefficient, with a value of 0.57 falls into the 'fair' category. The resulting accuracy values are influenced by several factors, such as GPS precision of 5-10 meters, while the drone-generated images have a spatial resolution of 3.98 cm, causing a potential discrepancy with the GPS data.

3.3. Sea urchin segmentation

Segmentation to map the distribution of sea urchins was performed by determining the threshold values for sea urchin pixels at each station. Prior to segmentation, contrast stretching image processing was performed to facilitate the interpretation of the sea urchin pixels. Contrast stretching brightens the values of the surrounding pixels, while reducing the values of the sea urchin pixels to make them darker and easily distinguishable from the surrounding environment. The results of contrast stretching are shown in **Fig 9**.

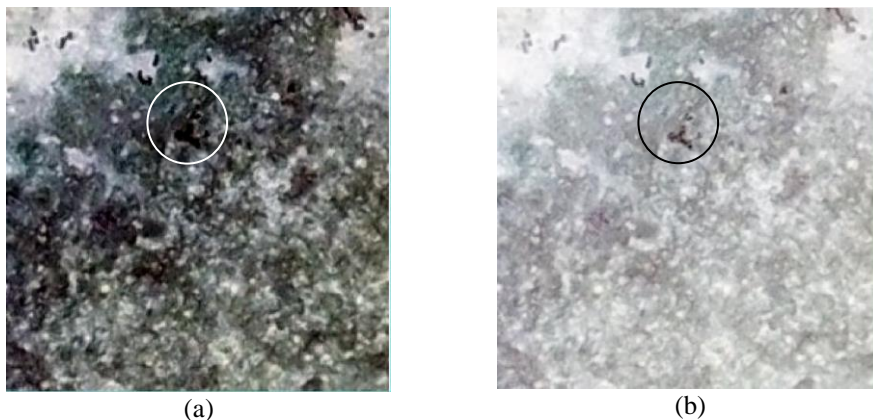


Fig 9. Results of contrast stretching. (a) before contrast stretching (b) after contrast stretching

Threshold values were obtained using the Cursor Value tool to determine the pixel values of sea urchins and their surrounding environments, enabling a clear separation. After obtaining the threshold values at each station, these values were converted to points using the Band Threshold to ROI tool available in the ENVI software. The sea urchin stations in the images are shown in **Fig 10**. The number of sea urchins per station at 10^2 m and the dominant benthic types at each station are shown in **Table 4**.

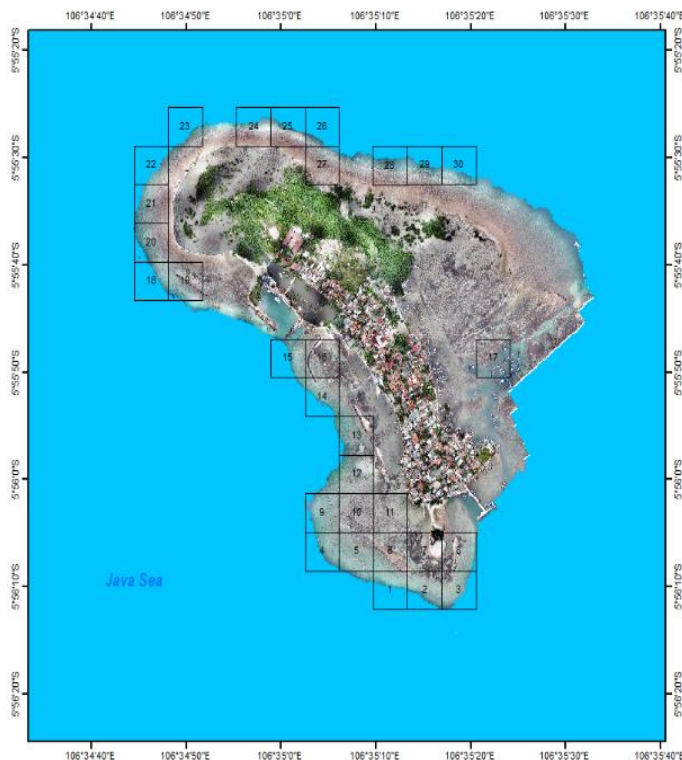


Fig 10. Aerial image of Lancang Island with 30 stations of sea urchin.

Table 4. Station dominant benthic type with sea urchin DN threshold and amount.

Station	Dominant	Threshold value (DN)	Amount
	Benthic type		
1	Sand	55-130	936
2	Living coral	70-120	2173
3	Sand	110-150	2348
4	Living coral	80-120	1105
5	Rubble	80-120	6650
6	Rubble	70-100	785
7	Sand	60-110	478
8	Sand	100-140	2453
9	Sand	100-130	992
10	Sand	51-110	10255
11	Rubble	80-110	3119
12	Rubble	70-105	3817
13	Rubble	60-110	4191
14	Rubble	60-110	1735
15	Rubble	60-110	2948
16	Rubble	60-110	1213
17	Rubble	60-100	355
18	Rubble	60-110	924
19	Rubble	70-120	5872
20	Rubble	60-100	2000
21	Sand	47-100	1689
22	Rubble	56-90	557

Station	Dominant	Threshold value (DN)	Amount
	Benthic type		
23	Rubble	40-70	174
24	Rubble	33-70	397
25	Sand	44-80	704
26	Sand	63-120	1236
27	Sand	37-80	722
28	Sand	42-90	711
29	Living coral	37-80	621
30	Living coral	35-60	389
Total			61551

3.4. Distribution of sea urchin with benthic habitat

The distribution of sea urchins within benthic habitats can be determined by overlaying the segmentation results of sea urchins from each station onto the benthic classification map. The distribution results for sea urchins in benthic habitats are shown in **Table 5**.

Table 5. The amount of sea urchin and density distribution in benthic habitat.

Benthic habitat	Benthic area (ha)	Sea urchin amount	Density (individual/ha)
Sand	18.555	17453	941
Seagrass	7.414	4383	591
Rubble	13.158	17865	1358
Living Coral	16.457	18094	1099
Dead Coral Algae	23.398	3756	161
Total	78.982	61551	4150

Based on **Table 5**, sea urchins are predominantly associated with rubble, sand, and living coral habitats. Sea urchins are commonly found in living coral habitats (18094 individuals). However, when considering habitat area, the highest density of sea urchins was rubble (1358 individuals/ha). According to a study by [28], sea urchins tend to inhabit coral reef ecosystems and seagrass beds. Furthermore, they tend to occupy substrates that consist of a mixture of sand and coral fragments. The distribution of sea urchins on Lancang Island,

Seribu Islands, and DKI Jakarta is predominantly in the western region of the island. In the eastern region of the island, there are several sea urchin stations typically located outside the reef, but there is one station inside the reef near the fishing platforms. Sea urchins on Lancang Island are distributed across five benthic classes (sand, rubble, seagrass, living coral, and dead coral algae). Benthic habitats generally provide shelter and food for sea urchins. Some benthic habitats also have mutually beneficial relationships with sea urchins. For instance, in living coral habitats, sea urchins find shelter and food and, in return, help maintain living corals by consuming excess algae.

4. Conclusion

The sea urchin distribution in the Lancang Islands, mapped using drones, showed that the most dominant sea urchins were found in the benthic habitat of living corals (18094 individuals). However, in terms of density, sea urchins were more abundant in rubble (1359 individuals/ha).

References

1. A. Padang, Nurlina, T. Tuasikal, R. Subiyanto, *Agrikan* **12(2)**, 220-227 (2019)
2. R.S. Steneck, *Developments in Aquaculture and Fisheries Science* **43**, 255-279 (2020)
3. B. Hereu, M. Zabala, C. Linares, E. Sala, *Marine Biology* **146**, 293-299 (2005)
4. B. Nababan, L.O.K. Mastu, N.H. Idris, J.P. Panjaitan, *Remote Sensing* **13 (4452)**, 1-23 (2021)
5. C.A. Sari, A.F. Syah, B. Prayudha, A. Salatalohi, *Jurnal Penginderaan Jauh Dan Pengolahan Data Citra Digital* **17(1)**, 33-42 (2019)
6. L.O.K. Mastu, B. Nababan, J.P. Panjaitan, *Jurnal Ilmu dan Kelautan Tropis* **10(2)**, 381-396 (2018)
7. C. Holness, T. Matthews, K. Satchell, E.C. Swindell, *International Geoscience & Remote Sensing Symposium (IGARSS)*, IEEE 6695-6698 (2016)
8. L. Tang, G. Shao, *Journal of Forestry Research* **26**, 791-797 (2015)
9. A.P. Colefax, P.A. Butcher, D.E. Pagendam, B.P. Kelaher, *Ocean & coastal management* **174**, 108-115 (2019)
10. S. Suryanti, S. Fatimah, Rudiyantri, *Buletin Oseanografi Marina* **9(2)**, 93-103 (2020)
11. A. Sugara, V.P. Siregar, S.B. Agus, *Jurnal Ilmu dan Teknologi Kelautan Tropis* **12(1)**, 135-150 (2020)
12. W.A. Febrina, I. Yarnuarsyah, A. Hudjimartsu, *Prosiding Seminar Nasional Teknologi Informasi* **2**, 354-358 (2019)
13. M.M.A. Lutfi, M.A. Machmud, *Jurnal Transformasi (Informasi & Pengembangan IPTEK)* **14(1)**, 1-13 (2018)
14. T. Y. Goh, S. N. Basah, H. Yazid, M. J. A. Safar, F. S. A. Saad, *Measurement* **114**, 298-307 (2018)
15. N. M. Zaitoun, M. J. Aqel, *Procedia Computer Science* **65**, 797-806 (2015)
16. S. D. Khirade, A. B. Patil, *International conference on computing communication control and automation*, 768-771 (2015)
17. E. Rahmani, I.W.G.A. Karang, I.D.N.N. Putra, *Journal of Marine Research and Technology* **5(1)**, 29-39 (2022)

18. J. Qin, M. Li, J. Zhao, D. Li, H. Zhang, J. Zhong, ISPRS Journal of Photogrammetry and Remote Sensing **207**, 298-311 (2024)
19. N. Dhanachandra, K. Manglem, Y. J. Chanu, Procedia Computer Science **54**, 764-771 (2015)
20. T. Kavzoglu, H. Tonbul, 8th International Conference on Recent Advances in Space Technologies (RAST), 113-117 (2017)
21. N.W. Prabowo, V.P. Siregar, S.B. Agus, Jurnal Ilmu dan Teknologi Kelautan Tropis **10(1)**, 123-134 (2018)
22. Trimble, *Ecognition developer: user guide*. Munchen, Germany: Trimble Germany GmbH 262 p (2014)
23. Y. Chen, Q. Chen, C. Jing, Journal of Spatial Science **66(2)**, 253-278 (2021)
24. S. Ghosh, A. Dasgupta, A. Swetapadma, 2019 International Conference on Intelligent Sustainable Systems (ICISS), 24-28 (2019)
25. N. E. Ramli, Z. R. Yahya, N. A. Said, Journal of Advanced Research in Applied Sciences and Engineering Technology **29(1)**, 256-265 (2022)
26. H. C. Kraemer, Wiley StatsRef: statistics reference online, 1-4 (2014)
27. S. S. Rwanga, J. M. Ndambuki, International Journal of Geosciences **8(4)**, 611-623 (2017)
28. A. Aziz, Oseana **19(4)**, 35-43 (1994)